Oxidation of Metals, Vol. 26, Nos. 3/4, 1986

Oxidation Kinetics, Breakaway Oxidation, and Inversion Phenomenon in 9Cr–1Mo Steels

A. S. Khanna,* P. Rodriguez,* and J. B. Gnanamoorthy*

Received January 7, 1986

The oxidation behavior of 9Cr–1Mo ferritic steels has been studied in air, oxygen, and steam at 1 atm pressure at various temperatures. Long-term experiments in air were carried out from 500–800°C by measuring the weight gains by interrupting the experiment at regular intervals of time. Short-term experiments in oxygen from 500–950°C and in air at 900 and 950°C were carried out by continuous recording of weight gain versus time in a continuous-recording thermogravimetric balance. Short-term experiments in steam were carried out using a special atmosphere furnace attached to the thermogravimetric balance. In air/oxygen, the weight gains at 700°C were lower than those at 600°C, while in steam, the weight gains at 800°C were lower than those at 700°C. This inversion phenomenon was observed for all the three steels viz. 9Cr–1Mo (high Si), 9Cr–1Mo (low Si), and 9Cr–1Mo–Nb steel. Examination of the oxide scales was carried out using SEM/EDAX, AES/ESCA, and X-ray diffraction techniques, and a mechanism is proposed for the occurrence of the inversion phenomenon.

KEY WORDS: oxidation kinetics; breakaway oxidation; inversion phenomenon; 9Cr–1Mo steel; 9Cr–1Mo–Nb steel; ferritic steels.

INTRODUCTION

9Cr–1Mo ferritic steels have become internationally accepted materials for several high-temperature applications.[1] The main interest for characterizing its oxidation behavior started, because of its extensive use as a cladding material in Advanced Gas-Cooled Reactors (AGR_s) in the U.K. In this

*Materials Development Laboratory, Reactor Research Centre, Kalpakkam-603102, India.

0030-770X/86/1000-0171$05.00/0

application, the material is used in an atmosphere of carbon dioxide. Detailed information about the compatibility of these steels in a carbon dioxide atmosphere is available in a recent conference proceeding.[2] The experimental work presented in the conference highlights two aspects, where the scope for additional work exists: (i) the accelerated test conditions showed that the material is susceptible to breakaway oxidation and (ii) the steel undergoes inversion phenomenon, i.e., it shows lower oxidation rate at a higher temperature compared to those at a lower temperature. Many workers[3,4,5] have attributed higher Si content as the cause of the inversion phenomenon. According to Taylor *et al.*,[5] a 9Cr-1Mo steel having a Si content of 0.69 wt.% or more shows inversion phenomenon, while a steel of lower content shows breakaway oxidation.

In order to confirm the role of Si in causing the inversion phenomenon, two steels of varying Si content were studied. This paper presents the results of the oxidation behavior of three 9Cr-1Mo steels viz. 9Cr-1Mo (high Si), 9Cr-1Mo (low Si), and 9Cr-1Mo-Nb stabilized steel. Studies in air and oxygen were carried out for all the three steels and in steam for the last two. From the results of the examination of the oxide layers formed, a mechanism for the inversion phenomenon is proposed.

EXPERIMENTAL PROCEDURE

The chemical composition of the steels studied is given in Table I. Steel having 0.47 wt.% of Si is designated as low-Si steel and those having 0.9 wt.% Si as high-Si steel.

9Cr-1Mo (low Si) and 9Cr-1Mo-Nb steels were received in the form of a cut-section of a boiler tube, 12 mm wall thickness. From this, $100 \times 10 \times 3$ mm thick strips were cut, cold-rolled to a thickness of 1 mm, sealed in evacuated quartz tubes and normalized at 950°C for 2 hr. 9Cr-1Mo (high Si) was received in the form of 1.5 mm thick strip which was rolled down

Table I. Chemical Compositions of the Steels Studied

	Wt.%								
Element	Cr	Mo	Mn	Si	P	S	C	Nb	Fe
9Cr-1Mo (high Si)	9.1	0.86	0.53	0.90	0.014	0.005	0.13	—	Bal
9Cr-1Mo (low Si)	8.70	1.0	0.53	0.47	0.012	0.008	0.11	—	Bal
9Cr-1Mo-Nb	8.46	1.02	0.46	0.41	0.001	0.004	0.083	0.072	Bal

to 1 mm thickness, and also normalized at 950°C for 2 hr. Rectangular coupons of surface area approximately 1 cm^2 were cut, polished to a fine-diamond finish, degreased, and washed in alcohol before use.

For air oxidation, the specimen after initial weighing was kept in a quartz boat and was exposed in a muffle furnace. Weight gains were measured by interrupting the experiment at regular intervals of time. Short-term experiments were carried out in a Mettler TA1 thermobalance (sensitivity 1 μg). Commercial oxygen purified from moisture and CO_2 was used for experiments carried out in oxygen atmosphere. A ramp heating programme with a heating rate of 25°C/min was used to reach the desired temperature. For kinetics measurements, the weight gain during heat up was neglected.

For experiments in steam, a special atmosphere furnace was attached to the Mettler TA1 thermobalance and weight gains were recorded continuously as a function of time. The description of the special atmosphere furnace is given elsewhere.[6]

Specimens after oxidation were examined using Scanning Electron Microscope (SEM) and Energy Dispersive X-ray Analysis (EDAX). Auger Electron Spectroscopy (AES) and Electron Spectroscopy for Chemical Analysis (ESCA) were carried out on a few air-oxidized samples. A few samples were analyzed for identifying the different layers on the cross-section of the scale.

EXPERIMENTAL RESULTS

Oxidation Kinetics

Oxidation in Air

Results of long-term exposure in air at 600–800°C and of short-term exposure in air at 900 and 950°C for 9Cr-1Mo (high Si), 9Cr-1Mo (low Si), and 9Cr-1Mo-Nb steel are given in Figs. 1, 2, and 3, respectively. For 9Cr-1Mo (high Si), the oxidation kinetics are in general logarithmic, in the sense that rapid initial growth is followed by a quiescent period. At 700°C, the oxidation kinetics in the initial stage is slower than those at 600°C. At 900°C, very little oxidation has occurred in the short duration of 6 hr and the kinetics appears to be linear in nature. At 950°C, the steel undergoes breakaway oxidation in about 30 min of exposure (Fig. 1).

9Cr-1Mo (low Si) shows much higher oxidation than 9Cr-1Mo (high Si) at all temperatures. At 600°C, the kinetics appears to be parabolic in nature in the initial stage. A sudden increase in oxidation rate is noted at around 400 hr exposure, after which there is again a parabolic oxidation. At 700°C the kinetics follow more or less a logarithmic law and the extent

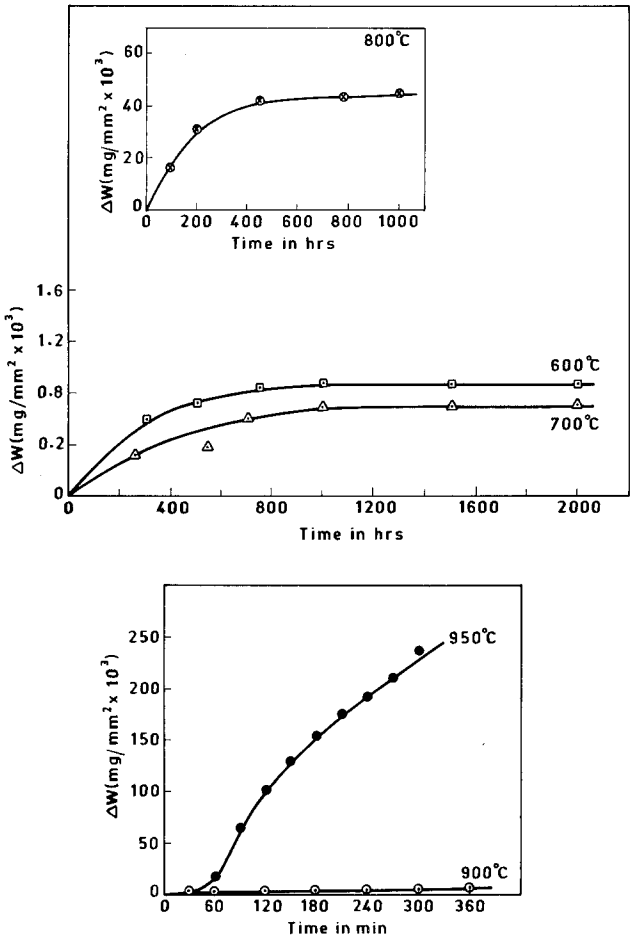

Fig. 1. Linear plots of weight gain vs time for 9Cr-1Mo (high Si) steel oxidized in air at various temperatures.

of oxidation is much smaller than those at 600°C. At 800°C, the kinetics appear to be logarithmic in the sense that the rapid initial growth is followed by a quiescent period. At 900 and 950°C, the steel undergoes breakaway oxidation even before the set temperature has been reached (Fig. 2).

The 9Cr-1Mo-Nb steel shows logarithmic kinetics at 600 and 800°C. At 700°C, the overall oxidation is lower than those at 600°C in the beginning, but after about 800 hr it becomes more than at 600°C. The kinetics at this temperature are approximately parabolic in nature. Oxidation behavior at 900 and 950°C is similar to that of 9Cr-1Mo (low Si). However, the

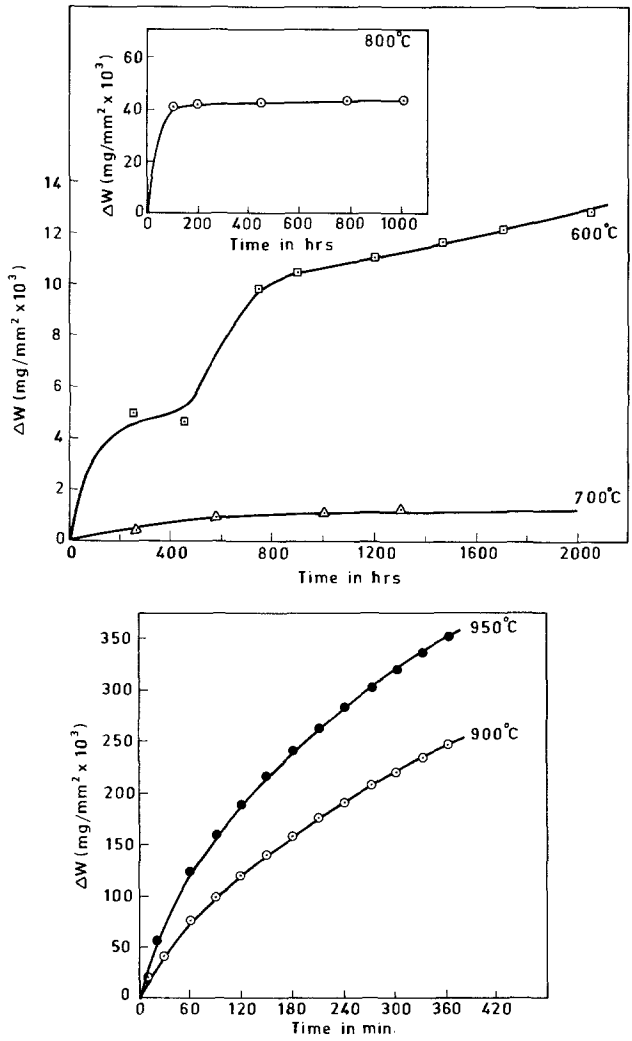

Fig. 2. Linear plots of weight gain vs time for 9Cr-1Mo (low Si) steel oxidized in air at various temperatures.

breakaway occurs just after reaching the set temperatures of 900 and 950°C. The post-breakaway linear rates of the three steels are listed in Table II.

From the results, it is evident that in the short-term exposure experiments the high-Si steel shows the highest resistance to breakaway oxidation and the low-Si, the least. A higher value for 9Cr-1Mo-Nb steel at 900°C appears to be an exception. At lower temperatures, one trend is common to all three steels; that is, the overall oxidation at 700°C is lower than those

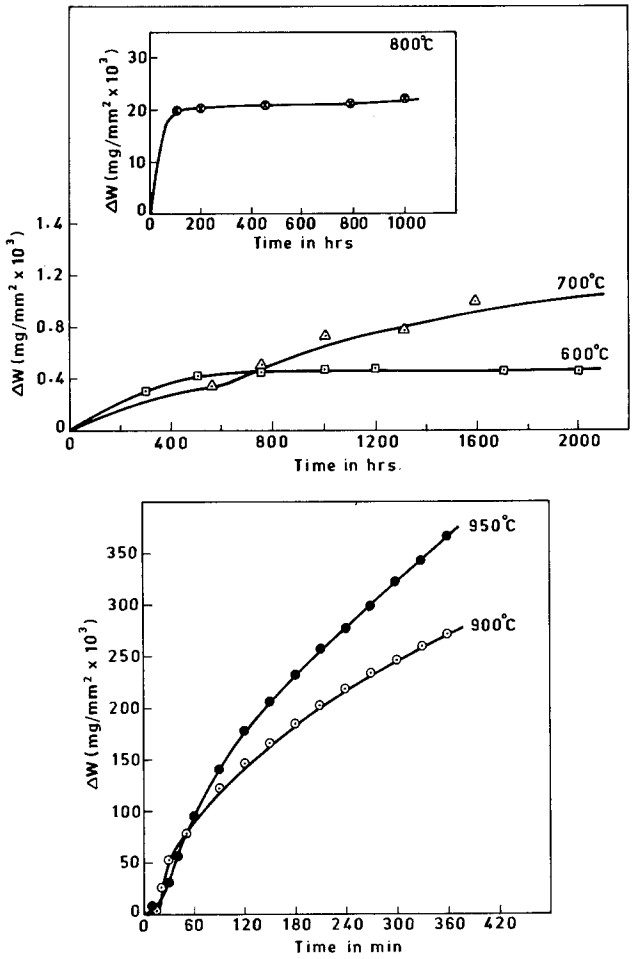

Fig. 3. Linear plots of weight gain vs time for 9Cr-1Mo-Nb steel oxidized in air at various temperatures.

Table II. Post-breakaway Oxidation Rates of Three 9Cr-1Mo Steels Oxidized in Air at Two Temperatures (g cm^{-2} sec^{-1})

Steel	900°C	950°C
9Cr-1Mo (high Si)	—	2.7×10^{-6}
9Cr-1Mo (low Si)	2.4×10^{-6}	4.6×10^{-6}
9Cr-1Mo-Nb	4.5×10^{-6}	3.6×10^{-6}

at 600°C. For 9Cr-1Mo-Nb, this is true in the beginning; the overall oxidation during long exposure is more than those at 600°C.

Oxidation in Oxygen

Results for 9Cr-1Mo (high Si), 9Cr-1Mo (low Si), and 9Cr-1Mo-Nb stabilized steels are given in Fig. 4a and 4b and 4c, respectively. The oxidation rate was very small at 500-800°C. The total weight gain was less than 1 μg for 24 hr-exposure tests in the case of 9Cr-1Mo (high Si) at temperatures of 500-800°C and in the cases of 9Cr-1Mo (low Si) and 9Cr-1Mo-Nb steels at temperatures of 500-700°C. Therefore, weight-gain rates at these temperatures have not been plotted. The oxidation rates for

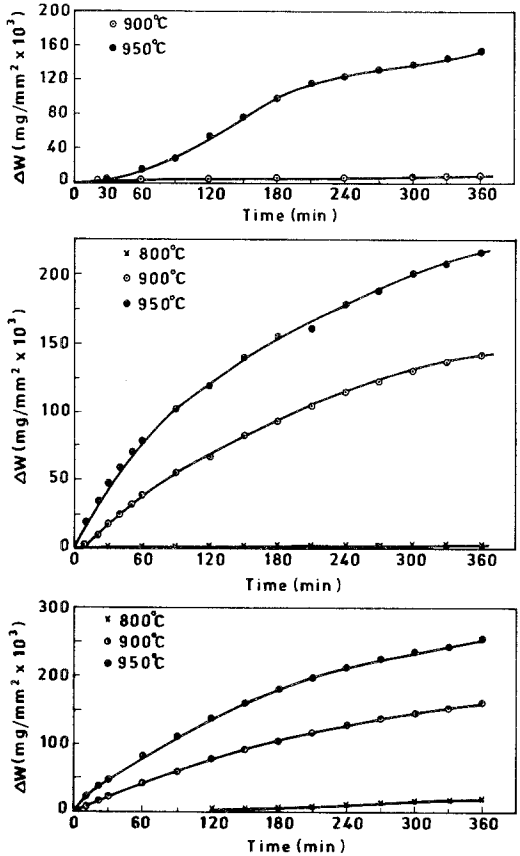

Fig. 4. Linear plots of weight gain vs time for (a) 9Cr-1Mo (high Si); (b) 9Cr-1Mo (low Si); and (c) 9Cr-1Mo-Nb stabilized steel in O_2 at various temperatures oxidized for a fixed duration of 6 hr.

9Cr-1Mo (high Si) at 900°C as well as for 9Cr-1Mo (low Si) and 9Cr-1Mo-Nb steels at 800°C were found to follow the logarithmic law. All three steels underwent breakaway oxidation at 900 and 950°C in this short-exposure time, except for 9Cr-1Mo (high Si) at 900°C. Both the 9Cr-1Mo (high Si) and 9Cr-1Mo-Nb steels underwent breakaway oxidation as soon as they reached these temperatures, while 9Cr-1Mo (high Si) steel underwent breakaway oxidation at 950°C after about 90 min exposure during which time it followed the parabolic rate law with $K_p = 0.045 \times 10^{-7}\ g^2\ cm^{-4}\ s^{-1}$.

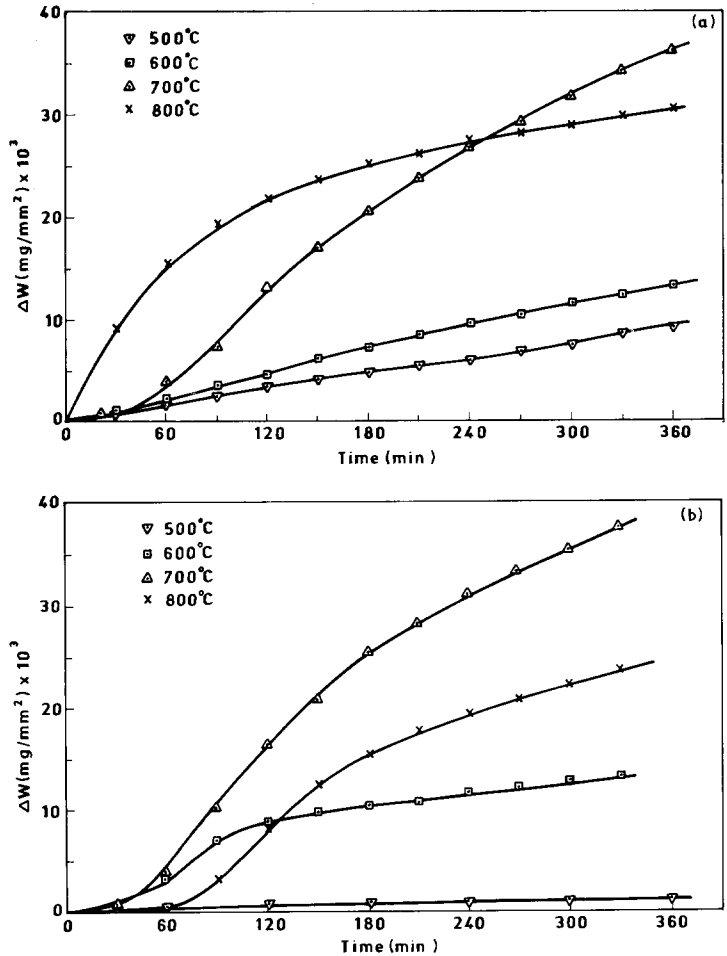

Fig. 5. Linear plots of weight gain vs time (a) 9Cr-1Mo (low Si) and (b) 9Cr-1Mo-Nb stabilized steel in steam at various temperatures oxidized for a fixed duration of 6 hr.

Table III. Parabolic Rate-Constants for the Oxidation of 9Cr-1Mo and 9Cr-1Mo-Nb Steel in Steam at Various Temperatures

Steel	Parabolic Rate-Constant K_p($g^2\ cm^{-4}\ sec^{-1}$) at			
	500°C	600°C	700°C	800°C
9Cr-1Mo (low Si)	5.5×10^{-11}	11.3×10^{-11}	7.0×10^{-10}	3.7×10^{-10}
9Cr-1Mo-Nb	0.63×10^{-12}	8.7×10^{-11}	9.2×10^{-10}	4.3×10^{-10}

The linear rate constants after the breakaway oxidation are 13.6×10^{-7} g cm^{-2} sec^{-1} for 9Cr-1Mo (high Si) at 950°C; 12.1×10^{-7} and 19.6×10^{-7} g cm^{-2} sec^{-1} for 9Cr-1Mo (low Si) respectively at 900 and 950°C; and 11.6×10^{-7} and 18.4×10^{-7} g cm^{-2} sec^{-1} for 9Cr-1Mo-Nb steel respectively at 900 and 950°C. In all cases the post-breakaway oxidation rate follows the parabolic rate law which is probably due to the formation of healing layers at the oxide/alloy interface.

Oxidation in Steam

The results of the kinetics studies in steam for 9Cr-1Mo (low Si) and 9Cr-1Mo-Nb steel are given in Fig. 5a and 5b, respectively. The oxidation rate follows parabolic kinetics at all temperatures studied from 500-800°C. The rate of oxidation is lower at 800°C compared to those at 700°C. The parabolic rate constants measured at these temperatures for these two steels are listed in Table III. Activation energies calculated using regression analysis in the temperature range 500-700°C are 20.8 and 28.0 KCal/mol for 9Cr-1Mo and 9Cr-1Mo-Nb, respectively.

Analysis of Oxide Scale

Surface Morphology

Results of the surface examination of 9Cr-1Mo (high Si) steel specimens oxidized in air/oxygen are given in Fig. 6a-6f at various temperatures. At 600°C, an iron-rich tarnishing layer was seen which was so thin that the underlying scratches due to polishing were also visible (Fig. 6a)). At 700°C, a few localized regions of excessive oxidation were seen, which when analyzed by EDAX, were found to be chromium-rich areas (Fig. 6b). The size and number of these chromium-rich regions increased respectively with an increase in temperature (Fig. 6c and 6d) and time (Fig. 6c and 6f). No significant change in surface morphology was noticed when the environment was changed from air to oxygen (Fig. 6d and 6e).

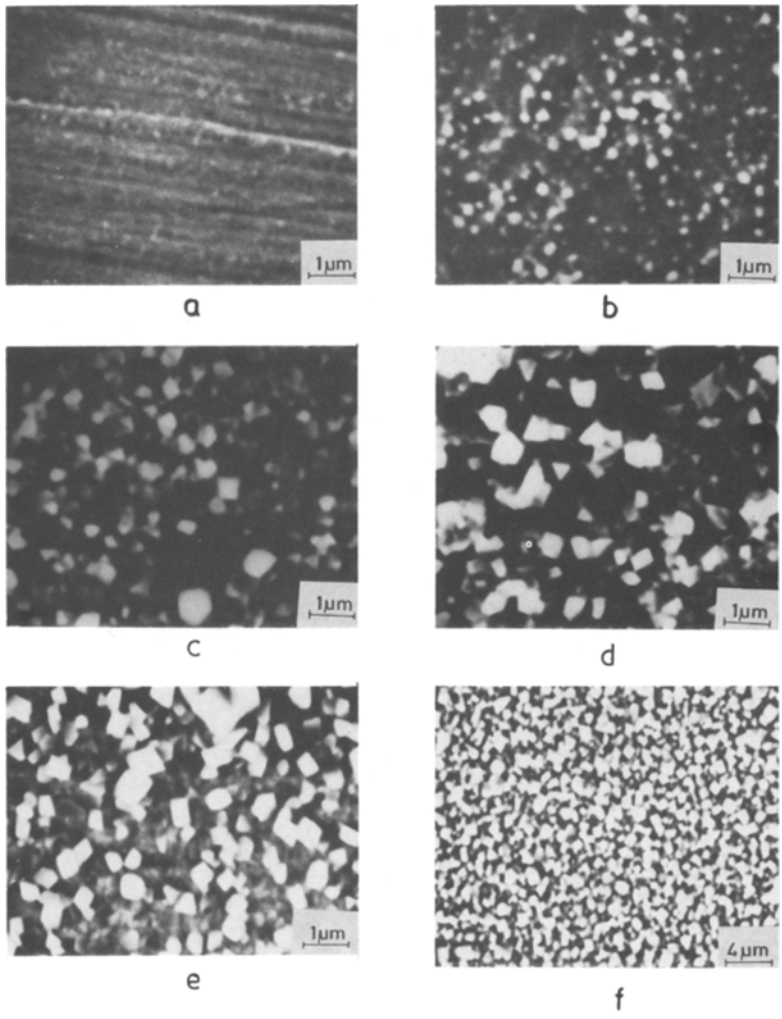

Fig. 6. SEM micrographs showing the morphology of oxide formed on 9Cr–1Mo steel oxidised at (a) 600°C for 6 hr in air; (b) 700°C for 6 hr in air; (c) 800°C for 6 hr in air; (d) 900°C for 6 hr in air; (e) 900°C for 6 hr in O_2; and (f) 800°C for 24 hr in air.

At 900°C, a uniform oxide layer rich in chromium was formed when oxidized for a short duration of 6 hr. Increasing the oxidation time to 24 hr, resulted in the excessive oxidation at the edges (Fig. 7a). The excessive oxidation at the edges was due to breakaway oxidation. The microstructure of the oxide scale at the edges is shown in Fig. 7b for oxidation in air and in Fig. 7c for oxidation in oxygen, respectively. Surface morphologies of

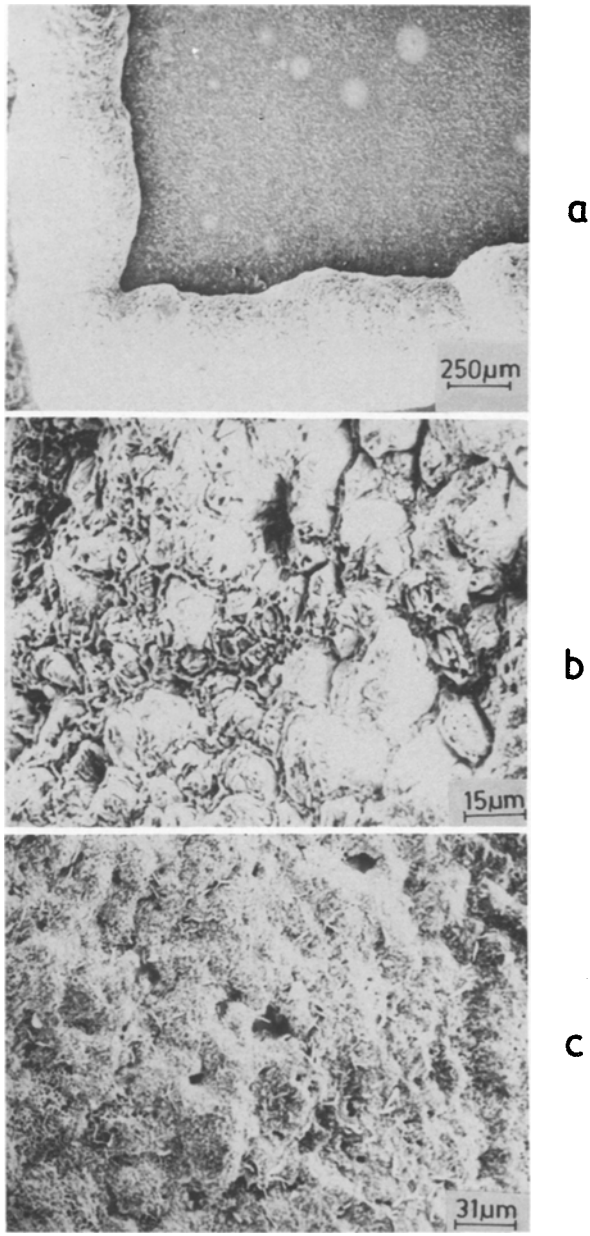

Fig. 7. SEM micrographs of the surface oxide formed on 9Cr–1Mo (high Si) steel oxidized at 900°C for 24 hr in air (a) showing protective oxidation on bulk surface and excessive (breakaway) oxidation at the edges; (b) and (c) showing breakaway oxidation at edges in air (b) and in oxygen (c).

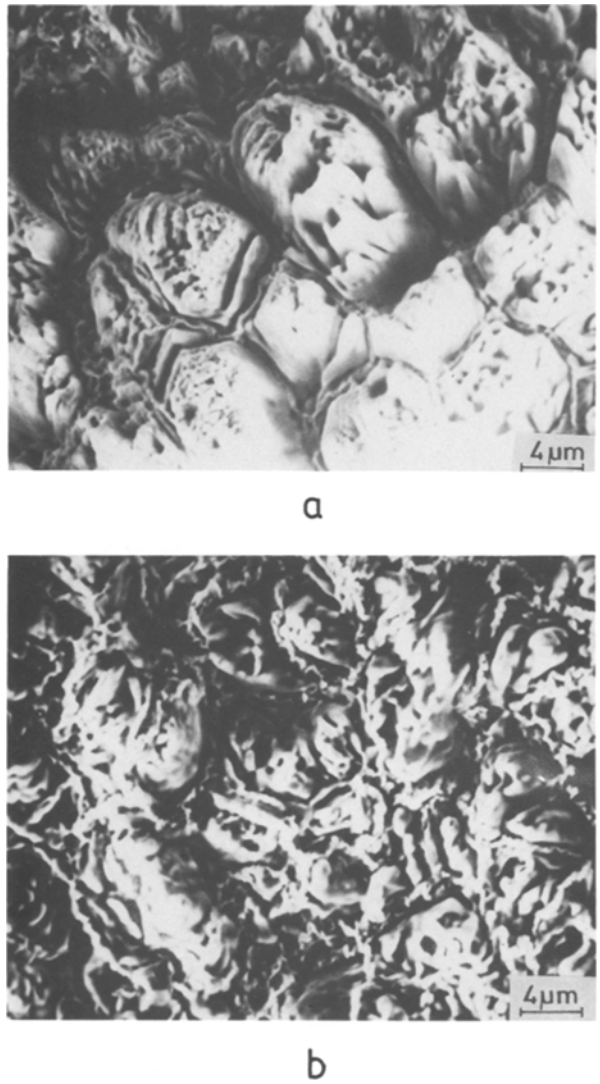

Fig. 8. SEM micrographs showing the breakaway oxidation on the oxide layer formed on 9Cr-1Mo (high Si) steel oxidized in (a) air (b) O_2 at 950°C for 6 hr.

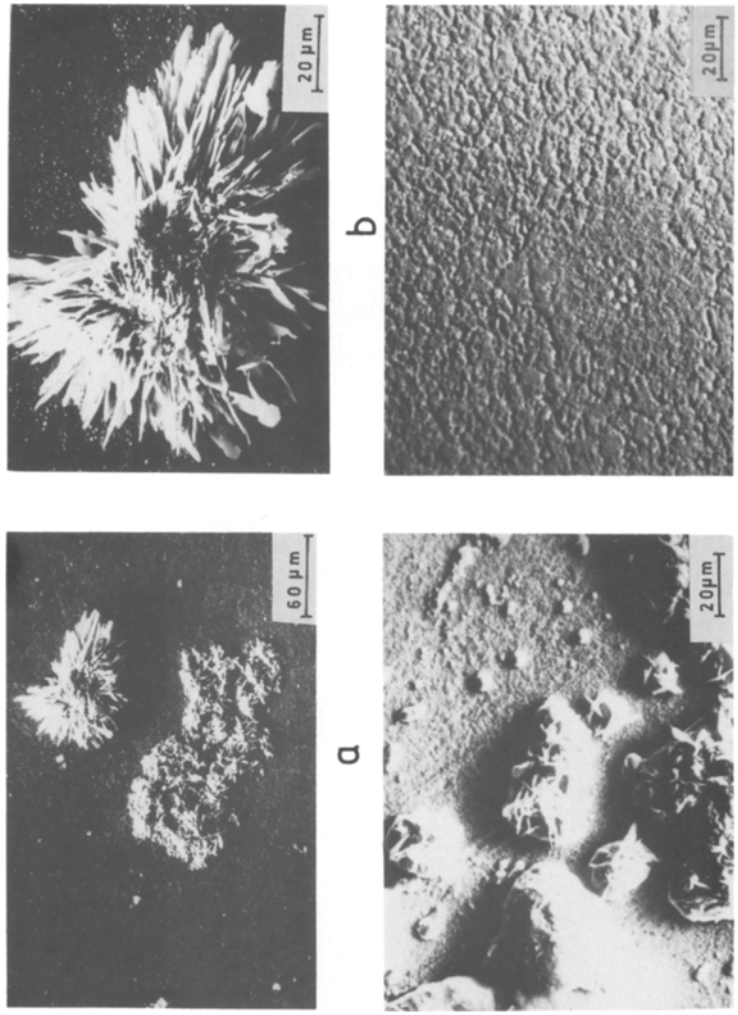

Fig. 9. SEM micrographs of (a) and (b) 9Cr-1Mo (high Si) steel; (c) 9Cr-1Mo (low Si) steel; and (d) 9Cr-1Mo-Nb stabilized steel oxidized in air for 2000 hr in air at 600°C.

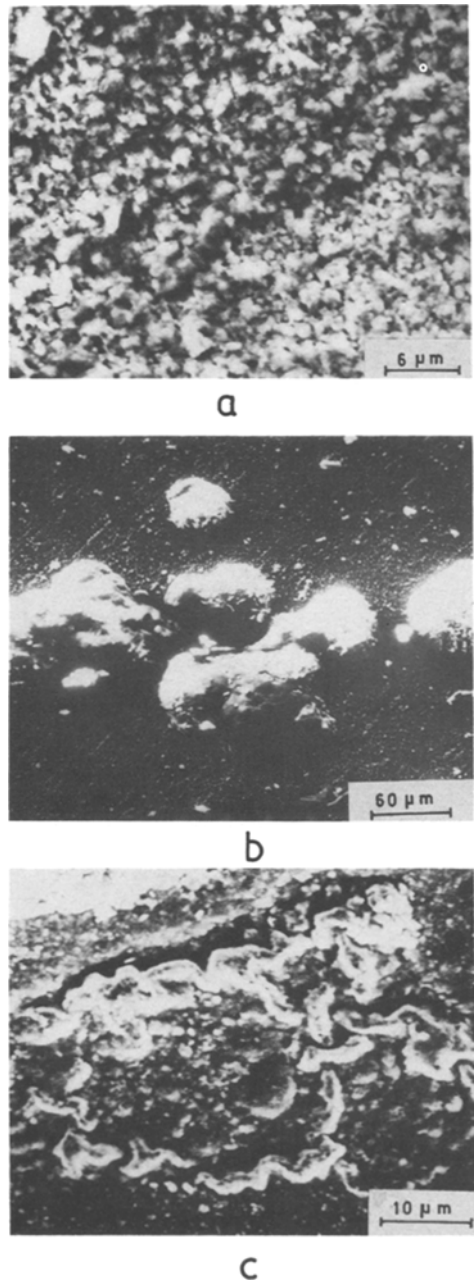

Fig. 10. Surface morphology of 9Cr–1Mo (low Si) steel oxidized in air at 700°C for 2000 hr (a) general morphology; (b) at high magnification; and (c) showing information of oxide loops at certain places.

the samples oxidized in air and oxygen at 950°C are shown in Fig. 8a and 8b, respectively. These microstructures are typical of breakaway oxidation.

SEM photomicrographs of the oxide scales on the three 9Cr-1Mo steels exposed in the long-term experiments are shown in Fig. 9a-d, respectively, for 9Cr-1Mo (high Si), 9Cr-1Mo (low Si), and 9Cr-1Mo-Nb steels. The general morphology is the emergence of nodules of oxides from localized areas of excessive oxidation in a uniform oxide scale. The size and number of these nodules are maximum on 9Cr-1Mo (low Si) steel and minimum on 9Cr-1Mo-Nb steel. 9Cr-1Mo (high Si) shows a "Sunflower" type morphology (Fig. 9b).

The morphology of the oxide formed on 9Cr-1Mo (low Si) steel at 700°C for an exposure of 2000 hr (Fig. 10) is in general similar to the oxide morphology at 600°C. The nodules formed are much smaller in size than those formed at 600°C (Fig. 9c). This is in agreement with the thermogravimetric results indicating a lower oxidation rate at 700°C compared to those at 600°C. In addition to the isolated nodules shown in Fig. 10b at a few locations, loops of grown oxides are visible (Fig. 10c).

Analysis of Scale Cross-Section

Figure 11 gives the cross-section of the scale on 9Cr-1Mo (high Si) steel, oxidized in air at 900°C. This shows excessive oxidation at the edges

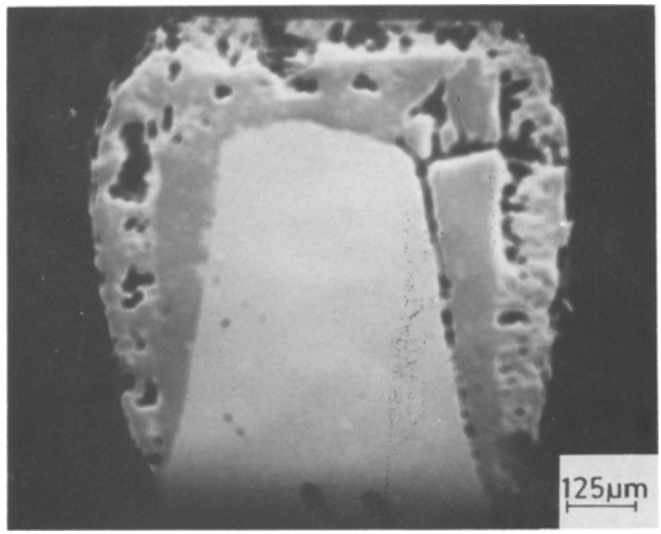

Fig. 11. SEM micrograph showing the scale cross-section at the edges of the 9Cr-1Mo steel (high Si) sample oxidized at 900°C for 24 hr in air.

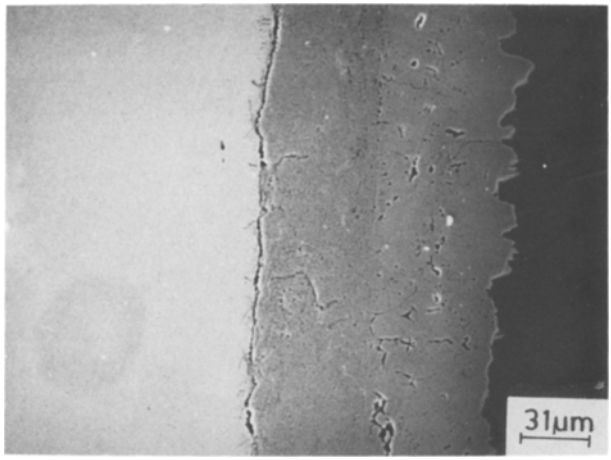

Fig. 12. SEM micrograph showing the scale cross-section of the oxide scale formed on 9Cr-1Mo (high Si) steel sample, oxidized in O_2 at 950°C for 6 hr.

as well discussed in an earlier section, while observing the surface morphology of the same sample. EDAX analysis confirmed that the bulk of the sample had a single layer rich in Cr possibly Cr_2O_3. At the edges a duplex layer was observed, an inner chromium-rich layer (possibly a Cr-rich spinel) and an outer iron-oxide layer. Figures 12 and 13 give the SEM micrographs of 9Cr-1Mo (high Si) steel oxidized at 950°C for 6 hr in oxygen and air, respectively. The scale formed in oxygen is comparatively thin, uniform, and has several cracks in the transverse direction. It is partially detached from the substrate. However, the scale formed in air is thicker. In addition to several cracks and voids, it has internal oxides in the alloy near the alloy/oxide interface (Fig. 13b). The scale is however adherent with the substrate, but has partially cracked from within, i.e., the outer scale has partially separated from the inner scale.

Detailed point-to-point analyses by EPMA were carried out for these samples, and the results are given in Table IV. The scale consists of an inner Cr-rich layer, probably of a spinel and an outer Fe_2O_3 layer.

Results of AES/ESCA Analyses

The oxide layers formed on 9Cr-1Mo steels during oxidation at 600-800°C were very thin. The scales formed were therefore analzed using AES and ESCA. Results are given in Figs. 14-18 for the oxidation of 9Cr-1Mo (high Si) steel in air at 600-900°C and in Figs. 19-22 for 9Cr-1Mo (low Si)

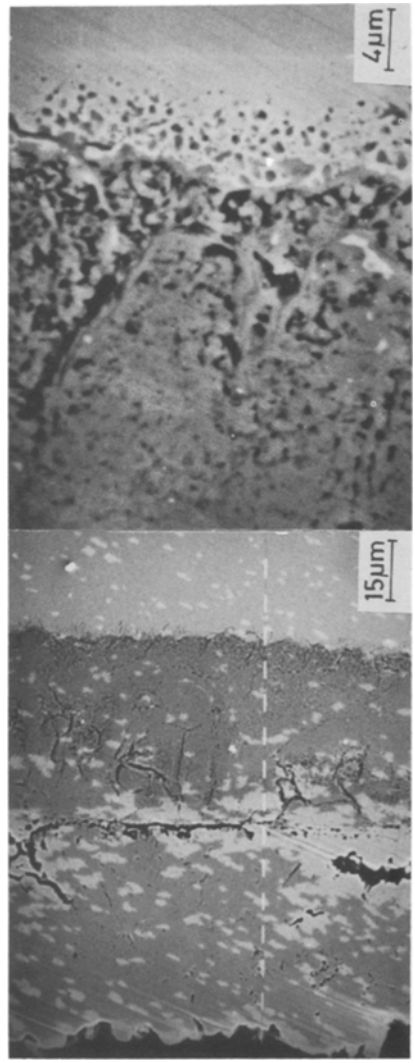

Fig. 13. SEM micrographs showing (a) the total scale cross-section (b) inner scale formed on 9Cr-1Mo (high Si) steel sample oxidized in air at 950°C for 6 hr.

Table IV. Analysis of Oxide Layer Using (EPMA) Formed on 9Cr-1Mo (High Si)

9Cr-1Mo steel oxidized under different conditions		Atom %		
		Fe	Cr	O
950°C, 17 hr air	Inner layer	30.30	9.73	60.00
	Outer layer	39.98	0.017	60.00
950°C, 6 hr O_2	Inner layer	30.1	8.95	60.00
	Outer layer	39.92	0.072	60.00
950°C, 6 hr air	Inner layer	29.94	10.05	60.00
	Outer layer	39.93	0.05	60.00

at 600-800°C. Results for the two steels do not differ much. These are summarised as follows:

600°C

The oxide surface seems to be iron-rich. Only traces of Cr are seen on the oxide surface. Depth profiles show that the oxide layer consists mainly

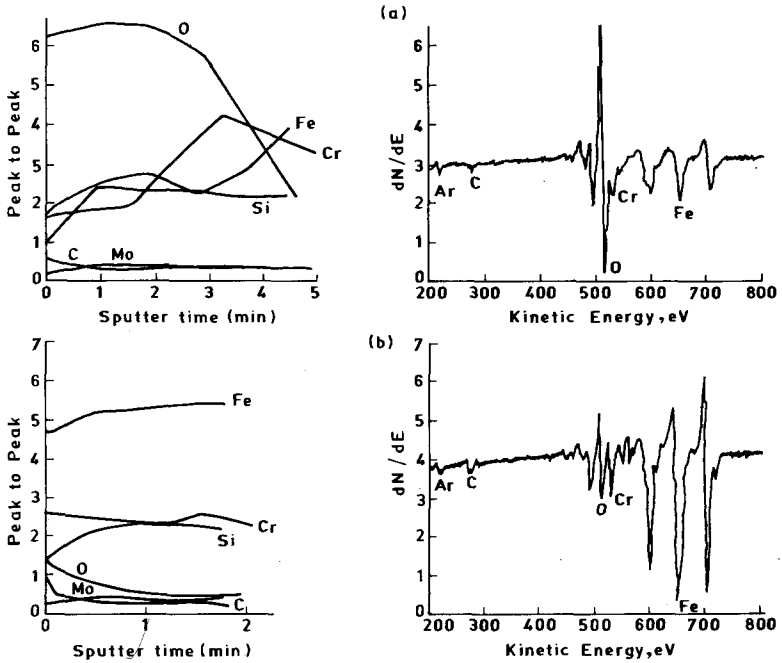

Fig. 14. AES depth profile and corresponding AES surface profiles for the air oxidized film formed on 9Cr-1Mo (high Si) steel at 600°C for 6 hr (a) for the first 5 min of sputtering (b) next 2 min of sputtering.

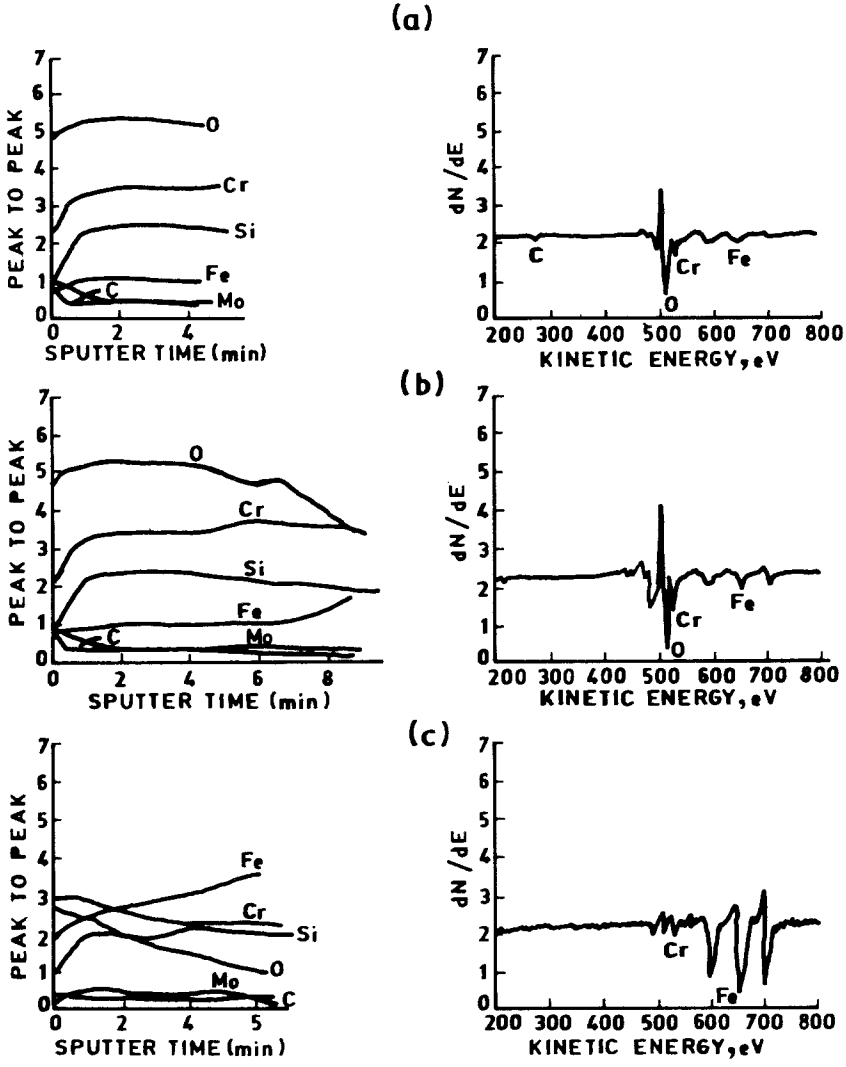

Fig. 15. Depth profiles and AES surface profiles of the oxide layer formed on 9Cr-1Mo (high Si) steel oxidized in air at 700°C for 6 hr (a) as received; (b) after 4 min; and (c) after 12 min of sputtering.

of iron. The main difference in the depth profiles of the two steels lies in the Si level. It can be seen that the Si level in the oxide layer of 9Cr-1Mo (high Si) steel is very high (Fig. 14) compared to that for 9Cr-1Mo (low Si) steel (Fig. 19a). Thus the high-Si steel contains considerable amount of Si in the oxide formed on it. The other striking difference is the thickness

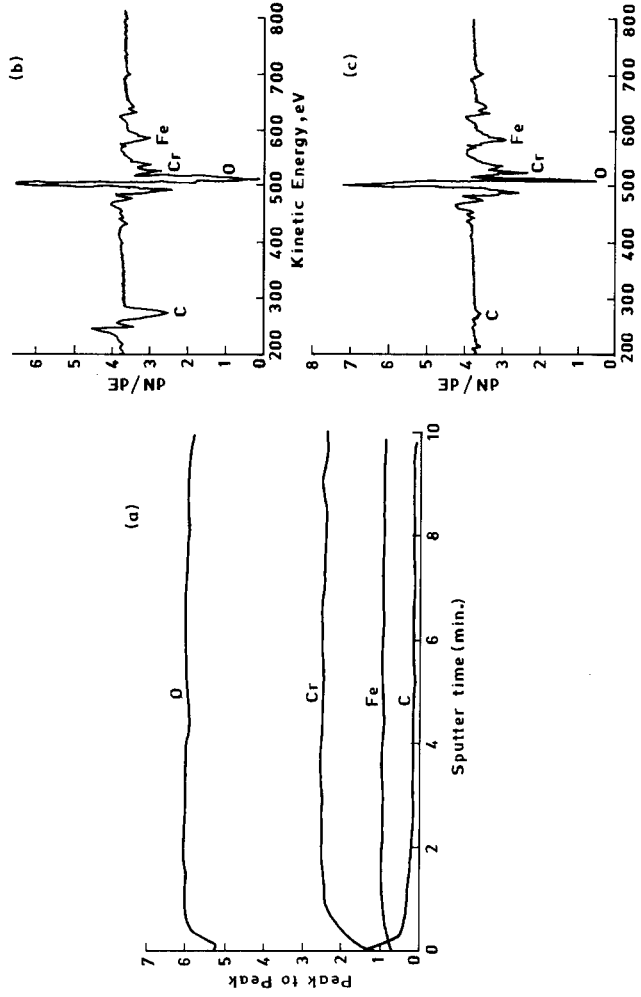

Fig. 16. (a) AES depth profile; (b) AES surface profile for initial surface; and (c) AES surface profile after 10 min sputtering for air oxidized film formed on 9Cr–1Mo (high Si) at 800°C for 6 hr exposure.

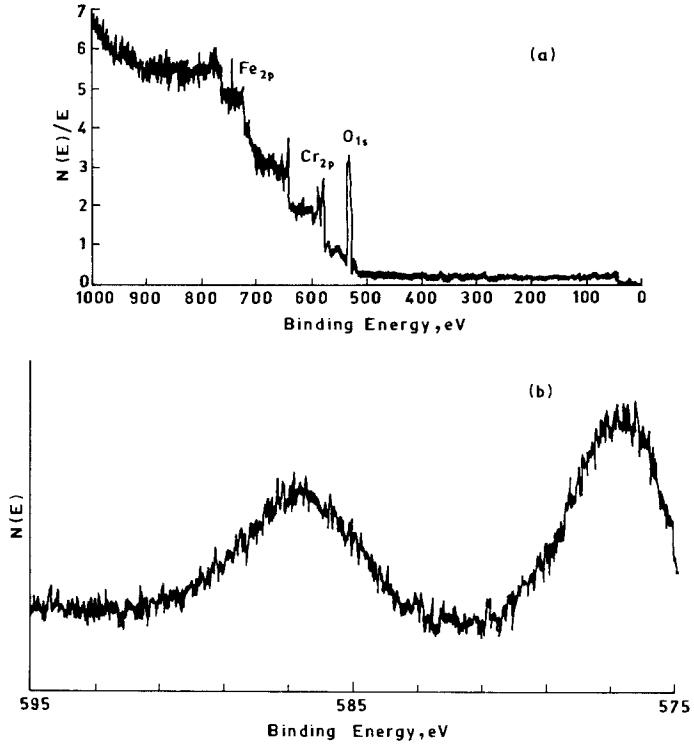

Fig. 17. (a) ESCA scan and (b) resolved ESCA Cr_{2p} peak for air oxidized 9Cr-1Mo steel sample at 800°C for 6 hr exposure.

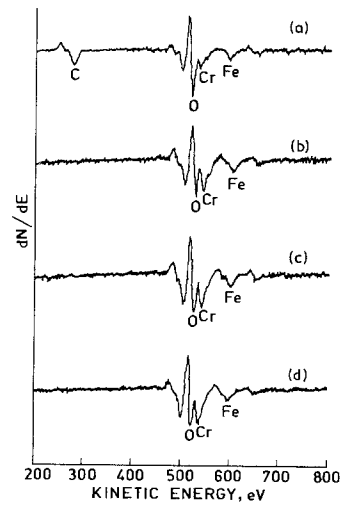

Fig. 18. AES surface profile on (a) initial surface; (b) after 5 min; (c) after 10 min; and (d) after 15 min of the sputtering of the oxide scale formed on 9Cr-1Mo (high Si) in air at 900°C for 6 hr exposure.

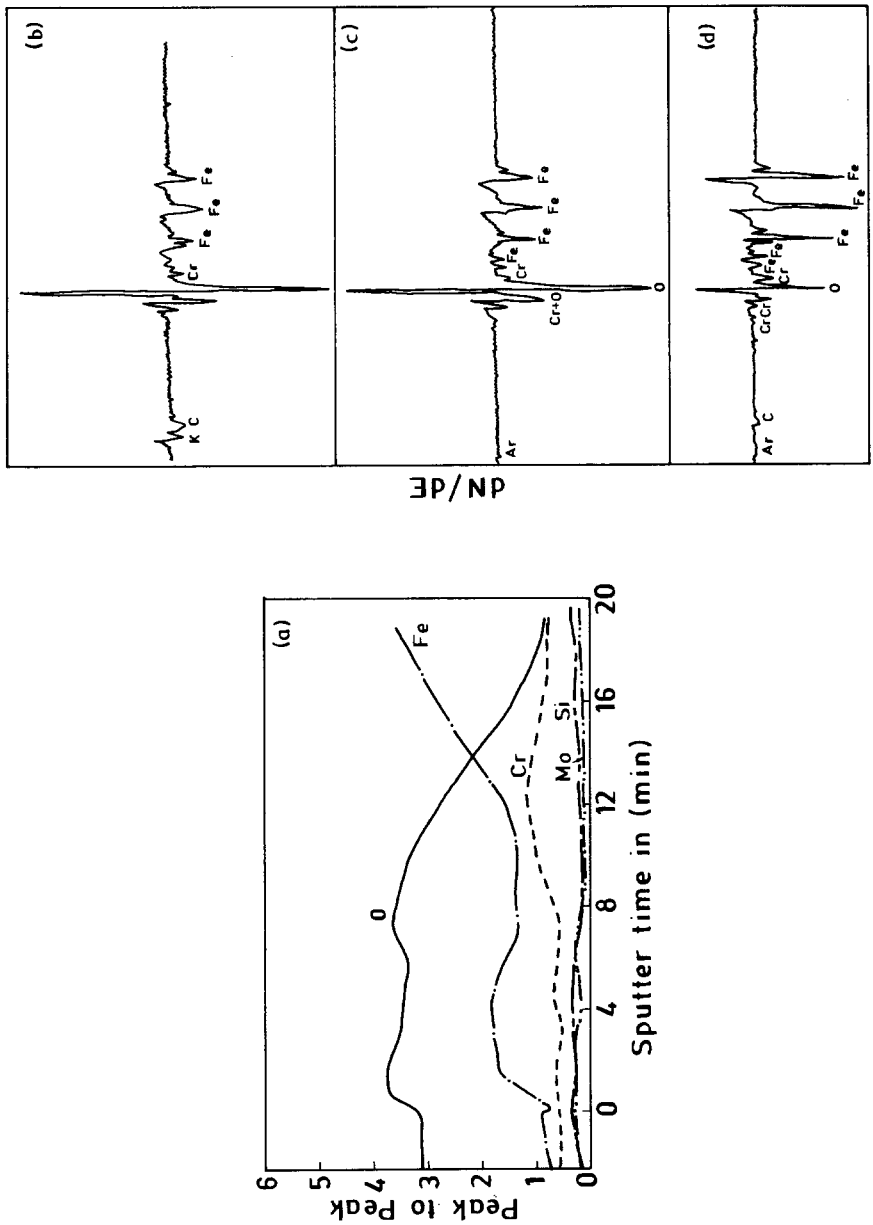

Fig. 19. (a) AES depth profile and AES surface profiles; (b) on as formed oxide; (c) after 8 min of sputtering; and (c) after 20 min of sputtering on 9Cr-1Mo (low Si) steel oxidized in air at 600°C for 6 hr.

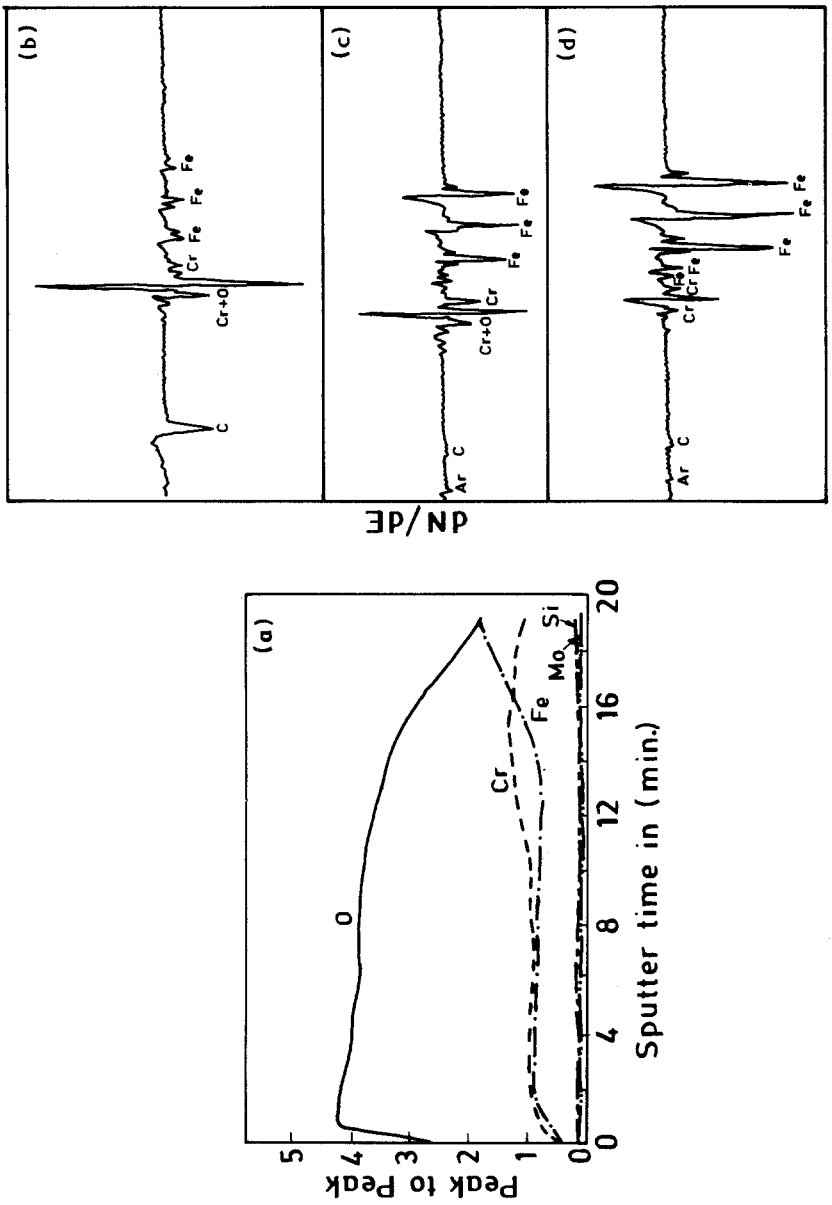

Fig. 20. (a) AES depth profile and AES surface profiles; (b) on as formed oxide surface; (c) after 20 min of sputtering; and (d) after 40 min of sputtering on 9Cr-1Mo (low Si) steel oxidized in air at 700°C for 6 hr.

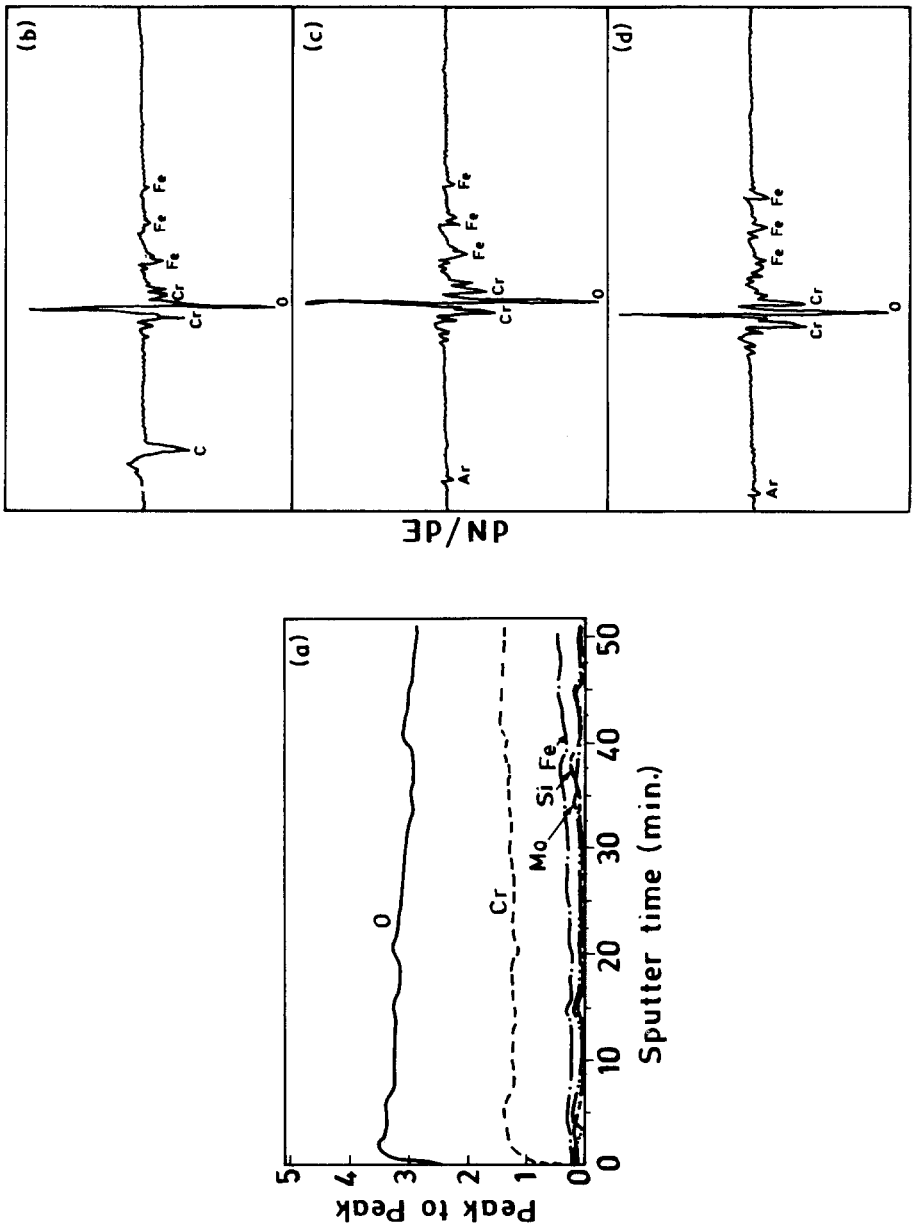

Fig. 21. (a) AES depth profile and AES surface profiles; (b) on as formed oxide; (c) after 8 min sputtering; and (d) after 50 min sputtering on 9Cr–1Mo (low Si) steel oxidized in air at 800°C for 6 hr.

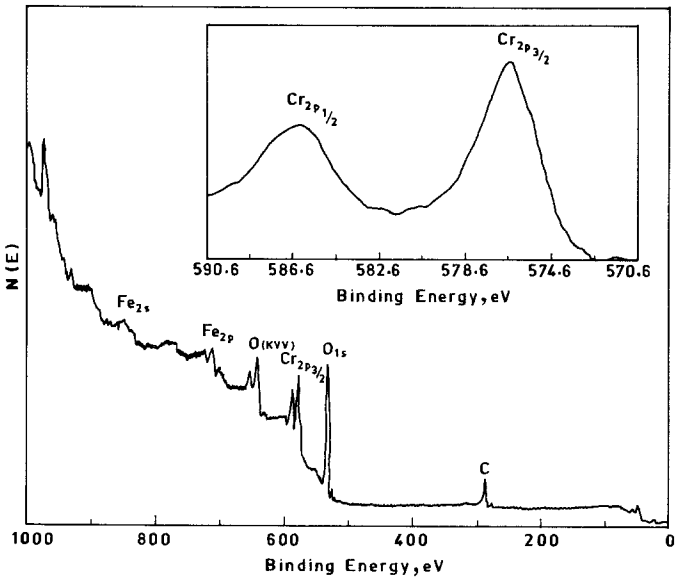

Fig. 22. (a) ESCA scan and (b) resolved Cr_{2p} peak for 9Cr-1Mo steel (low Si) sample oxidized in air at 800°C for 6 hr.

of the oxide layer. For the high-Si steel, the concentration of oxygen falls in about 3 min of sputtering, while for low Si steel this fall occurs after about 9 min. From this it is evident that the surface oxide on low Si alloy is about three times thicker than those on high Si steel. This is in conformity with the thermogravimetric results which show a much higher oxidation rate for low Si steels compared to those for high Si steel (Figs. 1 and 2).

700°C

Both AES surface profile curves and depth profile curves show prominent peaks of Cr on the surface oxide. Fe peaks are missing on the surface oxide profile. The Si level in the oxide layer is high in high-Si steel. The fall in the oxygen concentration starts in about 10 min of sputtering on the high-Si steel (Fig. 15b) compared to 12 min for the low-Si steel (Fig. 20a). Both the steels show a chromium-rich oxide layer on the surface.

800°C

Both the depth profiles and the surface profiles show a thick Cr-rich layer, which does not disappear even after 50 min of sputtering carried out on the low-Si steel (Fig. 21a). Scale identification was carried out using an ESCA run, the profiles for which are shown in Fig. 17a and 22a, respectively,

for high and low-Si steels. Both appear to be very much similar in nature. The Cr_{2p} peak when resolved further gave a prominent peak at 576.6 eV which is for Cr_2O_3. Resolved peaks are also exactly matching for the two alloys (Fig. 17b and 22b).

900°C

AES surface profiles at 900°C also indicate a Cr-rich oxide which is probably the same as at 800°C. The AES surface profiles measured after various sputtering times, show only a Cr peak. Traces of Fe are seen on AES profiles taken after 15 min of sputtering (Fig. 18).

DISCUSSION

Inversion phenomenon, i.e., a lower oxidation rate at higher temperature, compared to those at lower temperature, in 9Cr-1Mo steels has been reported by several workers.[4,5] This was attributed to the higher Si content in these alloys. Taylor *et al.*[5] found that the low-Si alloy, i.e., those having a Si content about 0.45 wt.% showed a higher oxidation rate at 600°C compared to those at 550°C. The rate at 600°C was an order of magntiude greater than those at 550°C. In the case of high Si alloys, i.e., those having a Si content between 0.64-0.78 wt.%, a significantly higher rate at 600°C was observed when compared with those at 500°C. In the case of steel having a Si content of 0.69 wt.%, the rate changed from 0.33 at 550°C to 0.28 mg cm^{-2} kh^{-1} at 600°C.[5] Based on the microprobe data obtained across the oxide/metal interface in the oxidized 9Cr-1Mo steel, Taylor *et al.*[5] suggested a possible critical role of Si either alone or more likely, coupled with local Cr in influencing the overall oxidation kinetics.

In the present study, three alloys having Si contents of 0.9 wt.% (high Si), 0.47 wt.% (low Si), and a stabilized 9Cr-1Mo-Nb steel having a Si content of 0.40 wt.% were used. A plot of dynamic weight change as a function of temperature (Fig. 23) showed a dip at 700°C. This was found in all three steels irrespective of their Si contents. This dip at 700°C was preceded by a higher weight gain at 600°C. This was further confirmed from the long-term oxidation tests carried out for these steels at these temperatures (Figs. 1, 2, and 3). All the steels (except 9Cr-1Mo-Nb steel exposed for more than 600 hr) showed a lower oxidation rate at 700°C compared to those at 600°C. Thus, the present results do not conform to the reported conclusion that only high-Si alloys show the inversion phenomenon. There is however a difference in the temperature at which the inversion takes place. This may be perhaps due to the different atmosphere used in the present investigations (the reported inversion by Taylor *et al.*[5] was found in a CO_2 atmosphere at about 600°C, while air/oxygen was used in the

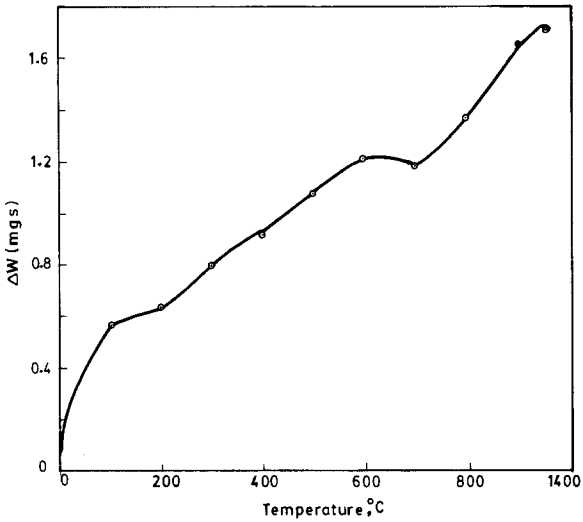

Fig. 23. Weight gain vs temperature plot for 9Cr-1Mo steel oxidized in air.

present study). Oxidation in a steam environment also confirms that the occurrence of inversion phenomenon is not confined to high-Si alloys and that the environment plays an important role in changing the temperature at which inversion occurs (e.g., 800°C in steam compared to 700°C in air/oxygen).

Detailed surface analysis using SEM/EDAX and AES/ESCA was carried out to arrive at the mechanism of the inversion phenomenon.

A fresh look at the surface morphological features of the oxide layer formed during 6 hr of oxidation of 9Cr-1Mo steel at temperatures ranging from 600-900°C, given in Fig. 6 is needed. The Fe/Cr ratio measured on the surface of the oxide formed is plotted as a function of temperature of exposure (Fig. 24). This shows a drop at 700°C, which coincided with the decrease in weight gain in the dynamic thermogravimetric run (Fig. 23) as well as with the appearance of Cr-rich phases on the surface of the sample oxidized at 700°C (Fig. 6b). Such Cr-rich phases are not present on samples oxidized at 600°C (Fig. 6a). When the diffusion coefficients of Cr in the steel at these temperatures are compared, it is seen that the diffusion coefficient of Cr at 700°C is about three orders of magnitude higher than those at 600°C.[7] This therefore leads to the conclusion that up to 600°C, the steel oxidizes to form a scale consisting of both Fe and Cr oxides, but at 700°C, the oxidation proceeds by the selective diffusion of Cr. It is obvious that an increase in the diffusion coefficient may lead to a decrease in the minimum concentration of the Cr required to form a selective oxide layer

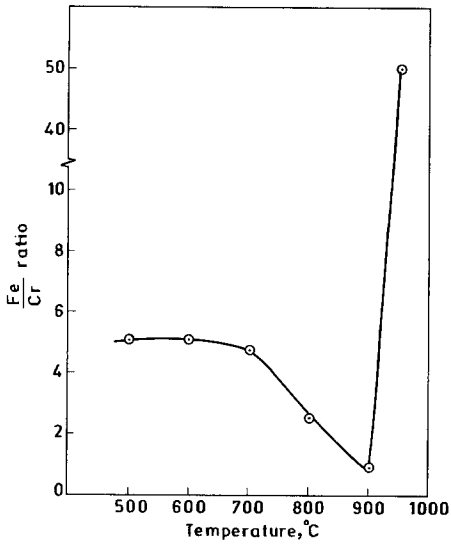

Fig. 24. Fe/Cr ratio of the surface oxides formed on 9Cr-1Mo (high Si) steel as a function of temperature.

on the steel, as per the equation[8]

$$N_B = \frac{V}{Z_B \, \mathrm{Mo}} (K_p/D)^{1/2}$$

where N_B is the minimum concentration required for selective oxidation, V is the molar volume of the alloy, Mo, the atomic weight of oxygen, K_p, the parabolic rate constant for oxidation and D, the diffusion coefficient of the element selectively oxidized. The subscript B refers to the element getting selectively oxidized.

According to this equation N_B is reduced by $D^{-1/2}$ times with an increase in D. Thus it is possible that under these conditions even a low-Cr steel oxidizes selectively. Further confirmation of the selective oxidation is available from the AES/ESCA results given previously. An iron-rich phase is formed at 600°C, while a thick Cr-rich layer is seen on samples oxidized at or above 700°C.

As reported earlier, the presence of Si definitely modifies the oxidation behavior. High-Si steels shows the lowest oxidation rate among the three steels. A high-Si steel resists breakaway oxidation up to about 6 hr at 900°C while both the other low-Si alloys undergo breakaway oxidation in about a few minutes after exposure at this temperature. There are two main theories

proposed by Wood[9] to explain the transition from a thin protective film to a stratified "non-protective" scale. Either the film is penetrated by the preferential diffusion of iron ions which form iron-oxides at the outer surface[10] or it is rendered "non-protective" by some form of cracking. According to the former theory, once a Cr_2O_3-rich scale is established on the specimen surface, the chromium concentration in the underlying substrate drops to some critical value, resulting in the internal oxidation of chromium and progressive diffusion of iron to form an external iron oxide layer.[11] This theory is able to explain the mechanism of breakthrough in the scale on 9Cr-1Mo steels, studied in the present work, since considerable Cr-depletion in the underlying alloy has been observed. However, the second theory cannot be ruled out altogether, i.e., the cracking of the oxide scale. This cracking could be due to the release of stresses, accumulated during the oxide growth[4,12] or due to ferrite/austenite transition suggested by Smeltzer[13] or due to any other reason. No evidence has however been obtained in the present investigations.

On the basis of the above discussion, the mechanism of oxidation of 9Cr-1Mo steels can be summarized, as shown schematically in Fig. 25.

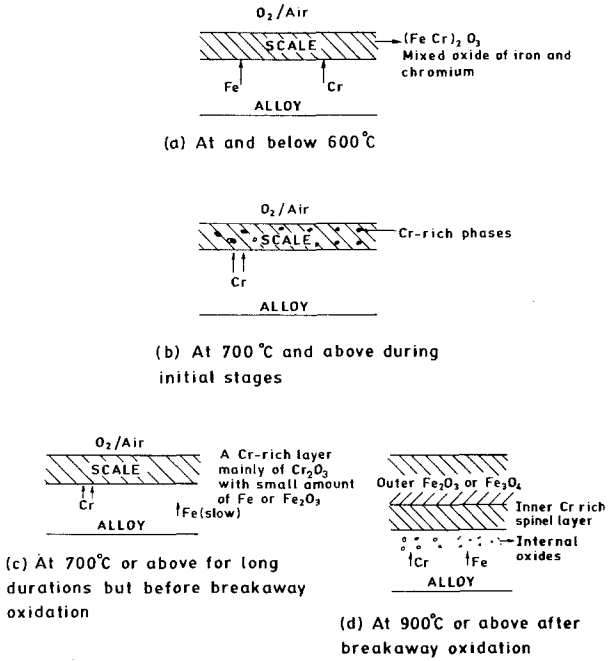

Fig. 25. Schematic of oxidation mechanism.

CONCLUSIONS

9Cr-1Mo steels oxidize without breakaway within a temperature range of 500-800°C studied for durations of 2000 hr at 500 and 600°C and for 1000 hr at 800°C. The alloys undergo breakaway oxidation in a short exposure of a few hours above 800°C. Among the three aloys, 9Cr-1Mo (high Si) has the lowest oxidation rate and 9Cr-1Mo (low Si), the highest. Further, the oxidation rates are more in air compared to those in oxygen.

For all three steels, the rate of oxidation is lower at 700°C compared to those at 600°C. The cause of this inversion is the switch over from general oxidation at 500 and 600°C to selective oxidation of Cr at 700°C and above. At 900 and 950°C, the breakthrough of the oxide scale occurs, through extensive chromium depletion in the underlying alloy which results in internal oxidation and transfer of vast quantities of iron to the scale to form stratified scales of outer Fe_2O_3 and inner spinel layer.

ACKNOWLEDGMENTS

The authors gratefully acknowledge the help rendered by Dr. K. L. Chopra and Dr. S. Rajagopalan of the Indian Institute of Technology and Dr. Lalit Kumar of the Bhabha Atomic Research Centre for their help in carying out AES/ESCA analyses and Shri S. Vaidyanathan of this Centre for carrying out SEM/EDAX analyses.

REFERENCES

1. J. Sanderson, in *Ferritic Steels for High Temperature Applications*, Ashok Khare ed. (Proc. Conf. ASM, 1983), p 78.
2. D. R. Holmes, R. B. Hill, and L. M. Wyatt, eds., *Corrosion of Steels in CO_2* (Proc. BNES, Reading 1974).
3. P. C. Rowlands, J. C. P. Garrett, F. G. Hicks, S. K. Lister, B. Lloyd, and J. A. Twelves, In *Corrosion of Steels in CO_2* D. R. Holmes, R. B. Hill, and L. M. Wyatt, eds. (Proc. BNES, Reading 1974), p 193.
4. D. R. Holmes, D. Mortimer, and J. Newell, in Ref. 3 p. 151.
5. J. W. Taylor and P. V. Trotsenberg, in Ref. 3, p. 180.
6. A. S. Khanna and J. B. Gnanamoorthy, *Trans. IIM* **38**, 147 (1985).
7. K. F. Smith, *Met. Sci.* **10**, 418 (1976).
8. G. C. Wood, *Oxid. Met.* **2**, 11 (1970).
9. G. C. Wood, *Corr. Sci.* **2**, 173 (1961).
10. J. O. Edstrom, *J. Iron Steel Inst.* **185**, 450 (1951).
11. G. R. Wallwork, *Reports on Prog. on Physics* **39**, 401 (1961).
12. V. R. Howes, *Corr. Sci.* **8**, 221 (1968).
13. W. W. Smeltzer, *Acta Met.* **8**, 268 (1960).